

# A *TFAP2C* Gene Signature Is Predictive of Outcome in HER2-Positive Breast Cancer



Vincent T. Wu<sup>1</sup>, Boris Kiriazov<sup>1</sup>, Kelsey E. Koch<sup>1</sup>, Vivian W. Gu<sup>2</sup>, Anna C. Beck<sup>1</sup>, Nicholas Borchering<sup>3</sup>, Tiandao Li<sup>1</sup>, Peter Addo<sup>1</sup>, Zachary J. Wehrspan<sup>4</sup>, Weizhou Zhang<sup>5</sup>, Terry A. Braun<sup>6</sup>, Bartley J. Brown<sup>6</sup>, Vimla Band<sup>7</sup>, Hamid Band<sup>7</sup>, Mikhail V. Kulak<sup>1</sup>, and Ronald J. Weigel<sup>1,2,4</sup>

## ABSTRACT

The AP-2 $\gamma$  transcription factor, encoded by the *TFAP2C* gene, regulates the expression of estrogen receptor- $\alpha$  (ER $\alpha$ ) and other genes associated with hormone response in luminal breast cancer. Little is known about the role of AP-2 $\gamma$  in other breast cancer subtypes. A subset of HER2<sup>+</sup> breast cancers with amplification of the *TFAP2C* gene locus becomes addicted to AP-2 $\gamma$ . Herein, we sought to define AP-2 $\gamma$  gene targets in HER2<sup>+</sup> breast cancer and identify genes accounting for physiologic effects of growth and invasiveness regulated by AP-2 $\gamma$ . Comparing HER2<sup>+</sup> cell lines that demonstrated differential response to growth and invasiveness with knockdown of *TFAP2C*, we identified a set of 68 differentially expressed target genes. *CDH5* and *CDKN1A* were among the genes differentially regulated by AP-2 $\gamma$  and that contributed to growth and invasiveness. Pathway analysis implicated the *MAPK13/p38 $\delta$*  and retinoic acid regulatory nodes,

which were confirmed to display divergent responses in different HER2<sup>+</sup> cancer lines. To confirm the clinical relevance of the genes identified, the AP-2 $\gamma$  gene signature was found to be highly predictive of outcome in patients with HER2<sup>+</sup> breast cancer. We conclude that AP-2 $\gamma$  regulates a set of genes in HER2<sup>+</sup> breast cancer that drive cancer growth and invasiveness. The AP-2 $\gamma$  gene signature predicts outcome of patients with HER2<sup>+</sup> breast cancer and pathway analysis predicts that subsets of patients will respond to drugs that target the MAPK or retinoic acid pathways.

**Implications:** A set of genes regulated by AP-2 $\gamma$  in HER2<sup>+</sup> breast cancer that drive proliferation and invasion were identified and provided a gene signature that is predictive of outcome in HER2<sup>+</sup> breast cancer.

## Introduction

The AP-2 transcription factor family plays a critical role in establishing clinically relevant patterns of gene expression in breast cancer. Expression of estrogen receptor- $\alpha$  (ER $\alpha$ ; encoded by the *ESR1* gene) is transcriptionally regulated in breast cancer (1), and AP-2 $\gamma$  (encoded by the *TFAP2C* gene) was identified as one of the key factors controlling *ESR1/ER $\alpha$*  gene transcription (2–6). In addition, AP-2 $\gamma$  regulates the expression of many other genes associated with the luminal breast cancer phenotype (4, 6, 7) and collaborates with FOXA1 and ER $\alpha$  in the transcriptional regulation of genes in hormone-responsive breast cancer (8). Within ER $\alpha$ -positive breast cancers, high levels of AP-2 $\gamma$  expression have been associated with poor patient survival and resistance to hormonal therapy (9, 10). Knockdown of *TFAP2C* in ER $\alpha$ -positive breast cancer cell lines repressed expression

of ER $\alpha$  and other markers of luminal breast cancer and induced markers associated with epithelial–mesenchymal transition (EMT) and the cancer stem cell phenotype (11). The highly homologous AP-2 family member, AP-2 $\alpha$  (encoded by the *TFAP2A* gene), was shown to regulate the expression of HER2 (12), which may function through several regulatory regions (13). Subsequent work suggested that AP-2 $\gamma$  contributes to HER2 gene regulation (14, 15), and an enhancer element has been described in the HER2 gene that is activated by AP-2 $\gamma$  (16).

The HER2<sup>+</sup> breast cancer subtype lacks ER $\alpha$  and progesterone receptor (PgR) expression with amplified HER2 expression and has a worse clinical course compared with the luminal breast cancer subtypes. However, even within the HER2<sup>+</sup> subtype of breast tumors, there is a high degree of heterogeneity (17). Detailed genetic analysis of HER2<sup>+</sup> breast cancers identified a subset displaying an addiction to *TFAP2C* gene amplification (18). For example, knockdown of *TFAP2C* in SKBR3 HER2<sup>+</sup> breast cancer cells reduced cell growth, and this dependency was associated with amplification of the *TFAP2C* gene locus. In contrast, other HER2-amplified cell lines failed to demonstrate reduced growth with knockdown of *TFAP2C*, suggesting a significant diversity in the pattern of genes regulated by AP-2 $\gamma$  in HER2<sup>+</sup> breast cancer. We sought to examine the regulation of genes by AP-2 $\gamma$  in HER2<sup>+</sup> breast cancers with the goals of characterizing differential AP-2 $\gamma$  target genes and defining pathways of gene regulation by AP-2 $\gamma$  that modulate cancer growth and progression.

## Materials and Methods

### Cell culture

Cell lines HCC1954, SKBR3, MCF-7, HCC202, HCC1569, and MDA-MB-453 were purchased from the ATCC, used at low (<10) passage number without further authentication or *Mycoplasma* testing, and propagated in the appropriate medium as recommended by the manufacturer. For experiments with all-*trans*-retinoic acid

<sup>1</sup>Department of Surgery, University of Iowa, Iowa City, Iowa. <sup>2</sup>Department of Molecular Physiology and Biophysics, University of Iowa, Iowa City, Iowa. <sup>3</sup>Department of Pathology, University of Iowa, Iowa City, Iowa. <sup>4</sup>Department of Biochemistry, University of Iowa, Iowa City, Iowa. <sup>5</sup>Department of Pathology, Immunology, and Laboratory Medicine, University of Florida, Gainesville, Florida. <sup>6</sup>Department of Biomedical Engineering, University of Iowa, Iowa City, Iowa. <sup>7</sup>Department of Genetics, Cell Biology and Anatomy, University of Nebraska Medical Center, Omaha, Nebraska.

**Note:** Supplementary data for this article are available at Molecular Cancer Research Online (<http://mcr.aacrjournals.org/>).

V.T. Wu and B. Kiriazov contributed equally to this article.

**Corresponding Author:** Ronald J. Weigel, University of Iowa, 200 Hawkins Drive, JCP 1509, Iowa City, IA 52242. Phone: 319-353-7474; Fax: 319-356-8378; E-mail: [ronald-weigel@uiowa.edu](mailto:ronald-weigel@uiowa.edu)

Mol Cancer Res 2020;18:46–56

doi: 10.1158/1541-7786.MCR-19-0359

©2019 American Association for Cancer Research.

(ATRA; Sigma, catalog no. 302-79-4), cells were grown in red-free media containing 10% charcoal-stripped FBS (Gibco, catalog no. F6765) to remove endogenous steroids. Cells were subsequently treated for 48 hours with concentrations 0.1 and 0.5  $\mu\text{mol/L}$  of ATRA or DMSO as a negative control.

### Gene knockdown

Cells were transfected using siRNA directed toward nontargeting #1 (NT Thermo Fisher Scientific, ID:4390843), *TFAP2C* (TFS, ID:107041), *CDH5* (TFS, ID:10509), *CDKN1A/p21* (TFS, ID: HSS173521), and *MAPK13* (TFS, ID: VHS40525) with Lipofectamine RNAiMAX reagent (Thermo Fisher Scientific, catalog no. 13778150), as per manufacturer's instructions. After 72 to 96 hours of incubation, cells were immediately analyzed or used in subsequent experiments. Cell clones of HCC1954 lines with stable knockdown of *TFAP2C* (Sigma, catalog no. TRCN0000019745) and negative control (Sigma, catalog no. SHC002) were generated using lentivirus-mediated shRNA cassette as described previously (11).

### Expression analysis

#### RNA

mRNA from cell lysates were obtained from cell lines using the RNeasy Mini Kit (Qiagen, catalog no. 74104) and converted to cDNA by quantitative PCR (qPCR) using random hexamers (Thermo Fisher Scientific) method. Using the  $\Delta\Delta C_t$  method of qPCR, relative gene expression was calculated using TaqMan primers to *TFAP2C* (TFS, catalog no.4331182, ID: Hs00231476\_m1), *CDH5* (TFS, catalog no. 4331182, ID: Hs00901465\_m1), *CDKN1A* (TFS, catalog no. 4331182, ID: Hs00355782\_m1), *MAPK11* (TFS, catalog no. 4331182, ID: Hs00177101\_m1), *MAPK12* (TFS, catalog no. 4331182, ID: Hs00268060\_m1), *MAPK13* (TFS, catalog no. 4331182, ID: Hs00234085\_m1), and *MAPK14* (TFS, catalog no. 4331182, ID: Hs01051152\_m1) with *GAPDH* (TFS, catalog no. 4331182, ID: Hs02758991\_g1), and 18s rRNA subunit (TFS, catalog no. 4331182, ID: Hs03003631\_g1) used as an endogenous control.

#### Western blots

Protein was isolated in RIPA lysis buffer (Millipore, catalog no. 20-188), supplemented with protease inhibitor (Roche, catalog no. 11836170001) and PhosSTOP (Roche, catalog no. 4906845001). The following primary antibodies were used according to the manufacturer's recommendations: AP-2 $\gamma$  1:700 (Abcam, catalog no. ab76007), VE-cadherin 1:1,000 (Cell Signaling Technology, catalog no. 2500), p21 1:700 (Cell Signaling Technology, catalog no. 2946), p38 MAPK 1:850 (Cell Signaling Technology, catalog no. 8690), p38 $\delta$ /*MAPK13* 1:1,000 (Cell Signaling Technology, catalog no. 2308), HER2/ErbB2 1:700 (Cell Signaling Technology, catalog no. 2165), and ER $\alpha$  1:700 (Millipore, catalog no. 04-820). *GAPDH* 1:2,000 (Santa Cruz Biotechnology, catalog no. sc-32233) was used as a loading control. Secondary antibodies were used according to the manufacturer's specification: anti-rabbit horseradish peroxidase (HRP) 1:5,000 (Cell Signaling Technology, catalog no. 7074), anti-mouse HRP 1:2,000 (Cell Signaling Technology, catalog no. 7076), and anti-goat 1:2,000 (TFS, catalog no. 31402). Protein was visualized with SuperSignal West Dura extended duration substrate (TFS, catalog no. 34075) and SuperSignal West Femto maximum sensitivity substrate (TSF, catalog no. 34095).

#### RNA sequencing

Experimental setup and analyses were performed in accordance to ENCODE Guidelines and Best Practices for RNA sequencing

(RNA-seq). *TFAP2C* knockdown was completed on HCC1954, SKBR3, and HCC1569 cell lines (biologic triplicates) using 96-hour siRNA transfection. RNA (100–200 ng/ $\mu\text{L}$ ) was harvested, knockdown confirmed with RT-PCR and protein Western blot analysis, frozen, and sent to the University of Nebraska (Omaha, NE) for further processing. The RNA quality was confirmed by the receiving facility and was subsequently sequenced (technical replicates specified by facility) with specifications for gene differentiation (50 base pair, single-end reads). Sequencing depth was adequate ( $\sim$ 50 million reads). Lentiviral shRNA knockdown of *TFAP2C* (Sigma, catalog no. TRCN0000019745) in HCC1954 was completed with RNA being sent to the same facility for sequencing (50 base pair, paired-end reads;  $\sim$ 75 million reads). The RNA-seq analysis of the raw data was performed using the Galaxy web platform at usegalaxy.org with the built-in tools: Bowtie2 for mapping and Cuffdiff for differential gene expression analysis, as recommended. For gene expression comparisons, genes with significant expression changes as determined by Cuffdiff data analysis were included. RNA-seq data are available at the GEO database (National Center for Biotechnology Information, Bethesda, MD) under accession number GSE126898.

#### Chromatin immunoprecipitation sequencing

Chromatin immunoprecipitation sequencing (ChIP-seq) was accomplished with AP-2 $\gamma$  antibody (Santa Cruz Biotechnology, catalog no. sc-12762) as described previously (7). ChIP-seq data are available in the GEO database (National Center for Biotechnology Information, Bethesda, MD) under accession number GSE126898.

#### Cell viability assay

Cells were plated on 96-well plates in technical quadruplicates. Ninety-six hours after siRNA transfection, cells were incubated with MTT (Thermo Fisher Scientific, catalog no. M6494) according to the manufacturer's recommended. Measurements were obtained on an Infinity 200 Pro (Tecan) plate reader at an absorbance of 570 nm. For cell counting, cells were plated on 96-well plates in technical quintuplicate. Ninety-six hours after siRNA transfection, cells were dyed with Trypan blue and counted using a hemacytometer.

#### Invasion assay

Invasion assay was performed using 24-well Transwell polycarbonate membranes (8.0- $\mu\text{m}$  pores; Corning Inc., catalog no. 353097), coated with 100  $\mu\text{L}$  Matrigel for 30 minutes at 37°C, washed with 500  $\mu\text{L}$  PBS, and  $1 \times 10^6$  cells plated in serum-free media 96 hours after siRNA transfection. Cells were loaded into an invasion chamber with growth factor-reduced Matrigel (Corning catalog no. 354230) diluted 1:10 in appropriate medium. After the 24-hour incubation, migrated cells were fixed and stained with 0.5% crystal violet for 20 minutes. The cells that had penetrated through the membrane were quantified under a microscope at  $\times 40$  magnification.

#### Regression analysis and model

Cox regression analysis was performed on expression values for 41-gene, 16-gene, and 3-gene panels from the Yau and colleagues (19) dataset. Expression values were obtained from the Xena cancer browser (20). Cox regression was performed using the "survival" package (version 2.38) in R (21). The Cox coefficients were used to determine "recurrence scores" (RS) as described by Paik and colleagues (22). Using the mean RS to separate patients into "low RS" and "high RS," we generated Kaplan-Meier (KM) survival curves to evaluate whether a combination of 41-gene, 16-gene, 3-gene panels, or "significant" ( $P \leq 0.05$ ) genes from the Cox regression conferred

Wu et al.

similar hazard or protection. The “survminer” package (version 0.4.3) in R was used for KM plots (23).

### Statistical analysis

Parametric data analysis and graphs were completed using the Student *t* test with GraphPad Prism 8.

## Results

As a first step to examining the role of AP-2 $\gamma$  in HER2<sup>+</sup> breast cancer, a panel of breast cancer cell lines was screened for the expression of AP-2 $\gamma$  with focus on HER2<sup>+</sup> breast cell lines (Fig. 1A). HCC1569, HCC202, SKBR3, HCC1954, and MDA-MB-453 were all confirmed to be ER $\alpha$ -negative with amplified expression of HER2. All of these cell lines expressed AP-2 $\gamma$  protein, although HCC202 had a significantly reduced level of expression. *TFAP2C* was knocked down in a panel of breast cancer cell lines using siRNA compared with a nontargeting (NT) siRNA (Fig. 1B) and was found to repress cell growth in MCF-7, HCC202, HCC1569, and SKBR3 (Fig. 1C). Although the effect on proliferation was significant in HCC202, the decrease in proliferation was modest, possibly due to the relatively low expression of AP-2 $\gamma$ . The findings in SKBR3 were

consistent with previously published data (18); however, knockdown of *TFAP2C* increased proliferation in HCC1954, consistent with previously published data that knockdown of *TFAP2C* in HCC1954 failed to repress proliferation (18). To confirm this finding, stable knockdown of *TFAP2C* was performed in HCC1954 using a lentiviral delivered shRNA, which significantly reduced expression of AP-2 $\gamma$  (Fig. 1B). HCC1954 cells with stable knockdown of *TFAP2C* (shHCC1954) were confirmed to have a significantly increased proliferative rate compared with cells with a NT shRNA (Fig. 1C). Previous studies in lung cancer reported that knockdown of *TFAP2C* enhanced cancer cell migration and invasion (24). Whereas knockdown of *TFAP2C* increased invasiveness in HCC1954, invasiveness was not significantly altered in SKBR3 (Fig. 2). These findings demonstrate that AP-2 $\gamma$  has differential effects on cell growth and invasiveness in HCC1954 and SKBR3 cell lines.

To identify the key AP-2 $\gamma$  target genes mediating cell growth and invasiveness, RNA-seq was used to characterize significant changes in gene expression with knockdown of *TFAP2C*. By RNA-seq analysis, knockdown of *TFAP2C* in HCC1954 with siRNA (compared with NT siRNA) identified 364 genes with significantly altered expression (Fig. 3). To further create specificity for AP-2 $\gamma$ -regulated genes and reduce possible “off-target” effects, RNA-seq analysis was performed

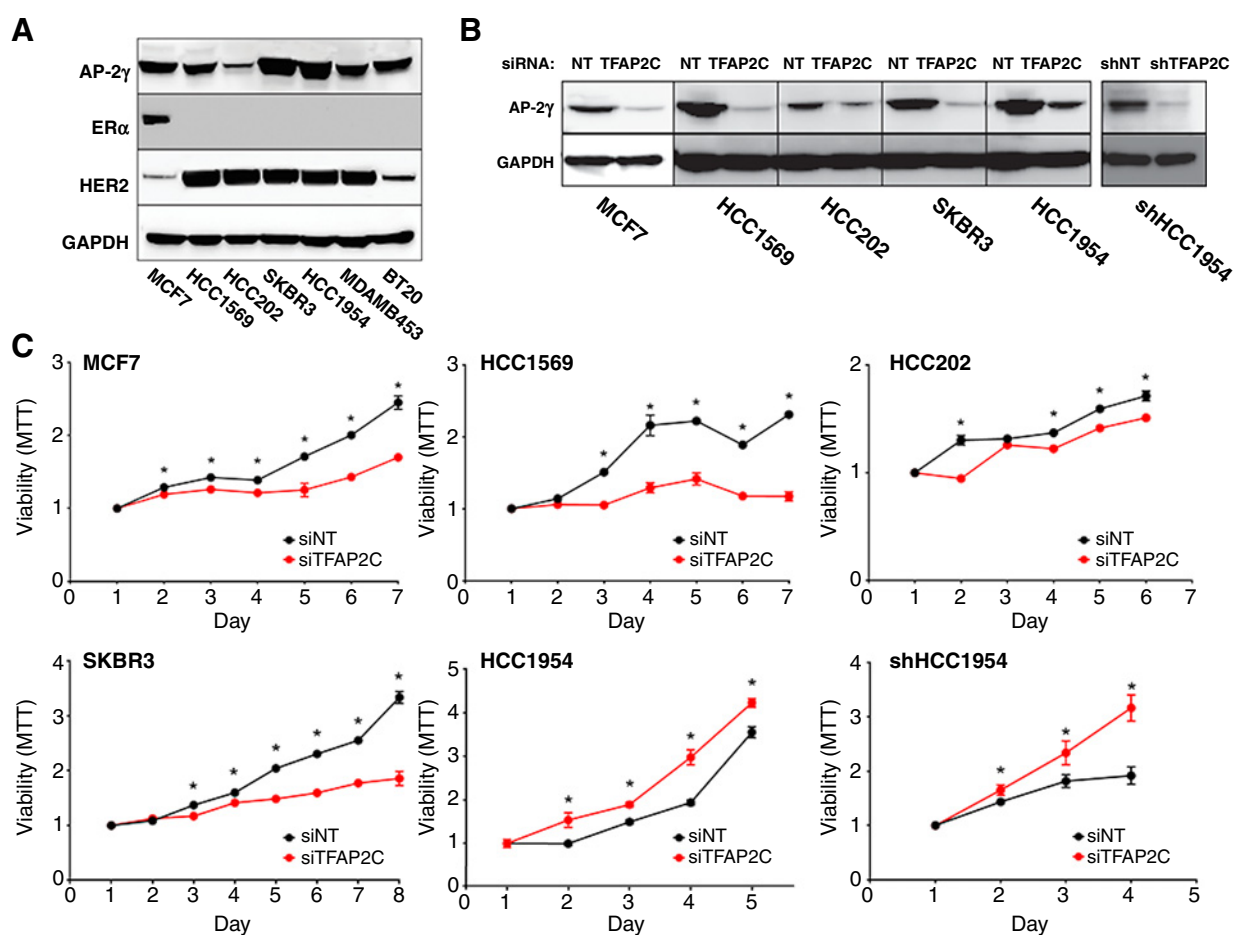
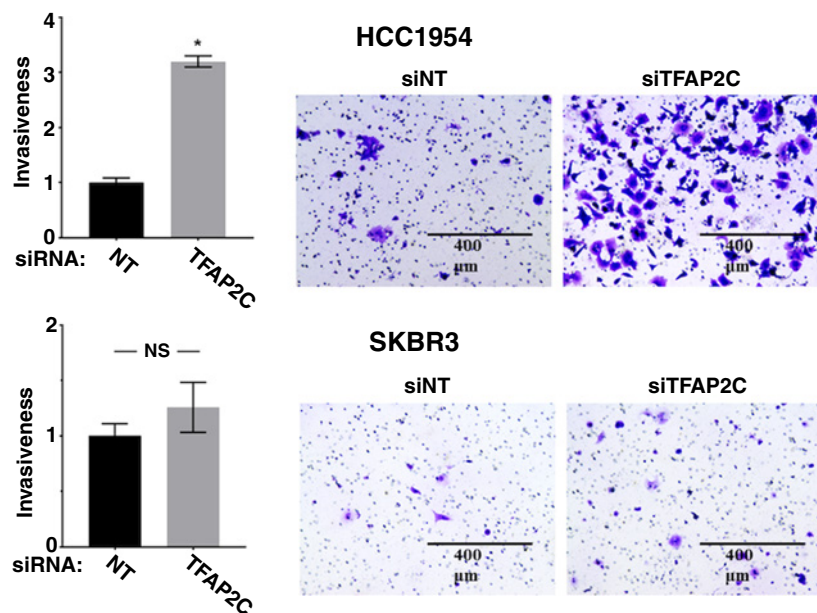


**Figure 1.**

Proliferative response with knockdown of *TFAP2C*. **A**, A panel of breast cancer cell lines was screened for expression of AP-2 $\gamma$ , ER $\alpha$ , and HER2. **B**, Knockdown of *TFAP2C* with siRNA and stable knockdown of *TFAP2C* with shRNA in HCC1954 cells. **C**, Proliferative response to knockdown of *TFAP2C* using MTT assay in cell lines indicated. \*, *P* < 0.05.

**Figure 2.**

Invasion assay in HCC1954 and SKBR3 with *TFAP2C* Knockdown. Graph showing relative cell invasiveness after knockdown of *TFAP2C* compared with NT siRNA in HCC1954 (top) and SKBR3 (bottom). Right, examples of cell invasion assay with knockdown of NT and *TFAP2C*. \*,  $P < 0.001$ .



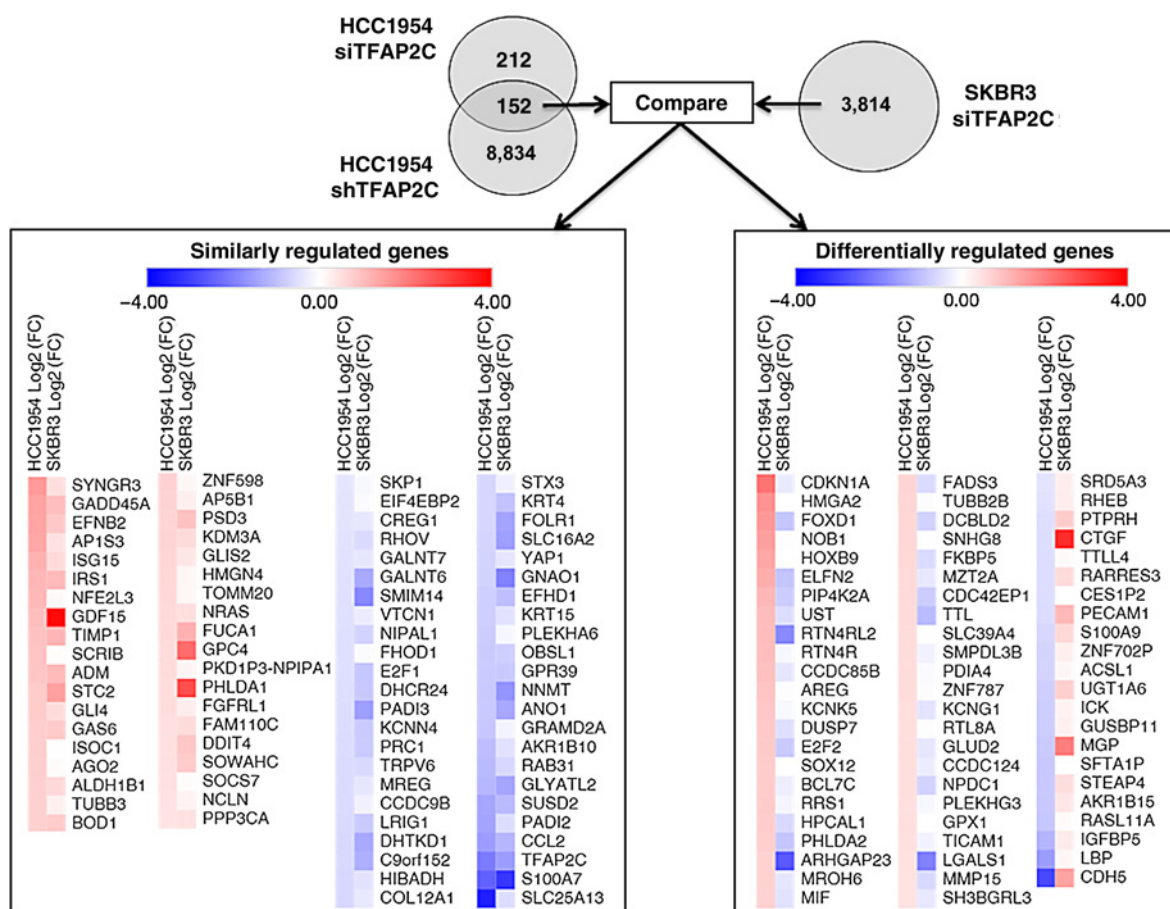
comparing expression in shHCC1954 with shTFAP2C versus shNT; this analysis identified 8,986 genes with significantly altered expression. A comparison of the two datasets yielded 152 AP-2 $\gamma$  target genes that were consistently altered with knockdown of *TFAP2C* by siRNA and shRNA in HCC1954 cells. Because HCC1954 demonstrated opposite growth regulation and invasiveness with knockdown of *TFAP2C* compared with SKBR3, we hypothesized that the AP-2 $\gamma$  target genes responsible for growth and invasion would be differentially regulated with knockdown of *TFAP2C* in HCC1954 versus SKBR3. Hence, RNA-seq analysis was performed in SKBR3 after knockdown of *TFAP2C* with siRNA; in this analysis, a total of 3,814 genes were significantly altered. The pattern of expression for the 152 AP-2 $\gamma$  target genes identified in HCC1954 was subsequently compared with expression changes in SKBR3. Of note, only 79 of the 152 *TFAP2C* target genes in HCC1954 were found to change expression significantly in the RNA-seq dataset from SKBR-3. However, important physiologic differences could be due to genes that display significant changes in HCC1954 only. When examining the pattern of expression for all 152 AP-2 $\gamma$  target genes in HCC1954 and SKBR3, 84 genes were noted to change in the same direction (Similarly Regulated Genes, Fig. 3, left). Within the set of similarly regulated genes, 38 genes increased and 46 genes decreased with knockdown of *TFAP2C*. Particularly reassuring was the finding that expression of the *TFAP2C* gene demonstrated the third most significant decrease in expression in both cell lines. Differential regulation was found for 68 genes; 46 genes had increased expression in HCC1954 and decreased in SKBR3, whereas 22 genes had decreased expression in HCC1954 and increased in SKBR3.

More detailed analysis was focused on the 68 AP-2 $\gamma$  target genes that changed in different directions (differentially regulated genes, Fig. 3, right) in HCC1954 compared with SKBR3 with knockdown of *TFAP2C*. Selected Western blots were performed to demonstrate changes in protein levels that confirmed the RNA-seq data (Fig. 4 A–C). Within the dataset for HCC1954, *CDKN1A* had the greatest increase in expression and *CDH5* had the greatest decrease. Western blots confirmed that vascular endothelial cadherin (VE-cadherin; encoded by the *CDH5* gene) decreased in HCC1954 and increased in SKBR3, whereas, p21 (encoded by the *CDKN1A* gene)

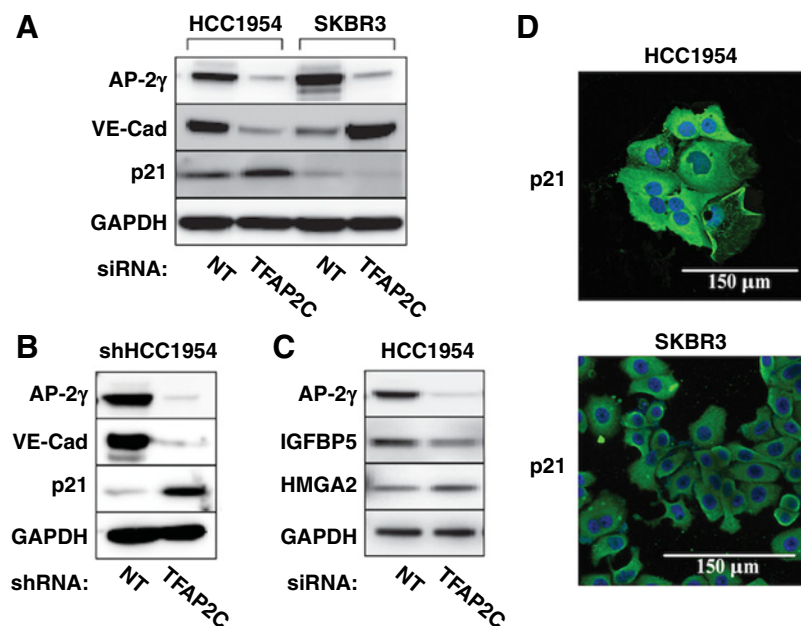
increased in HCC1954 and decreased in SKBR3 with knockdown of *TFAP2C*. Identical changes in VE-cadherin and p21 were found in shHCC1954 cells with *TFAP2C* knockdown compared with shNT (Fig. 4B). Additional Western blots for IGFBP5 and HMGA2 with knockdown of *TFAP2C* in HCC1954 cells further confirmed the validity of the RNA-seq results (Fig. 4C); these proteins were not consistently identified in protein extracts from SKBR3 (data not shown). Immunofluorescence staining with anti-p21 confirmed cytoplasmic localization (Fig. 4D), which is consistent with previous findings in HER2-positive cell lines (25).

Further attempts were made to establish the role of specific AP-2 $\gamma$  target genes in regulating cell growth and invasion. Because *CDKN1A* was induced by knockdown of *TFAP2C* in HCC1954, *TFAP2C* was knocked down with or without cknockdown of *CDKN1A* and proliferation was assessed by counting viable cells (Fig. 5). Knockdown of *CDKN1A* reduced cell growth and partially reversed the growth-stimulatory effects of *TFAP2C* knockdown. Assessment of proliferation in parallel experiments using MTT assay gave identical results (Supplementary Fig. S1A). Because knockdown of *TFAP2C* in HCC1954 was associated with increased cell invasiveness, the role of p21 in altering invasiveness was also assessed. Knockdown of *CDKN1A* alone did not alter invasiveness; however, knockdown of *CDKN1A* reversed the increase in invasiveness noted with knockdown of *TFAP2C* (Fig. 5). In parallel experiments in SKBR3 cells, *CDH5* was knocked down with and without cknockdown of *TFAP2C*. Interestingly, knockdown of *CDH5* alone had no significant effect on cell proliferation (Fig. 5) and similar findings were demonstrated when proliferation was assessed by MTT assay (Supplementary Fig. S1B). However, knockdown of *CDH5* partially rescued the reduction in cell proliferation induced by knockdown of *TFAP2C*. This finding suggests that part of the growth-suppressive effects induced in SKBR3 through loss of AP-2 $\gamma$  is mediated by *CDH5* upregulation. Knockdown of *TFAP2C* with cknockdown of *CDH5* in SKBR-3 confirmed no significant effect on invasion, though there was a slight reduction in invasiveness with knockdown of *CDH5* that failed to reach statistical significance ( $P = 0.12$ ; Fig. 5). These findings support the conclusion that regulation of *CDH5* and *CDKN1A* contribute to alterations of proliferation and invasiveness induced by knockdown of *TFAP2C*.

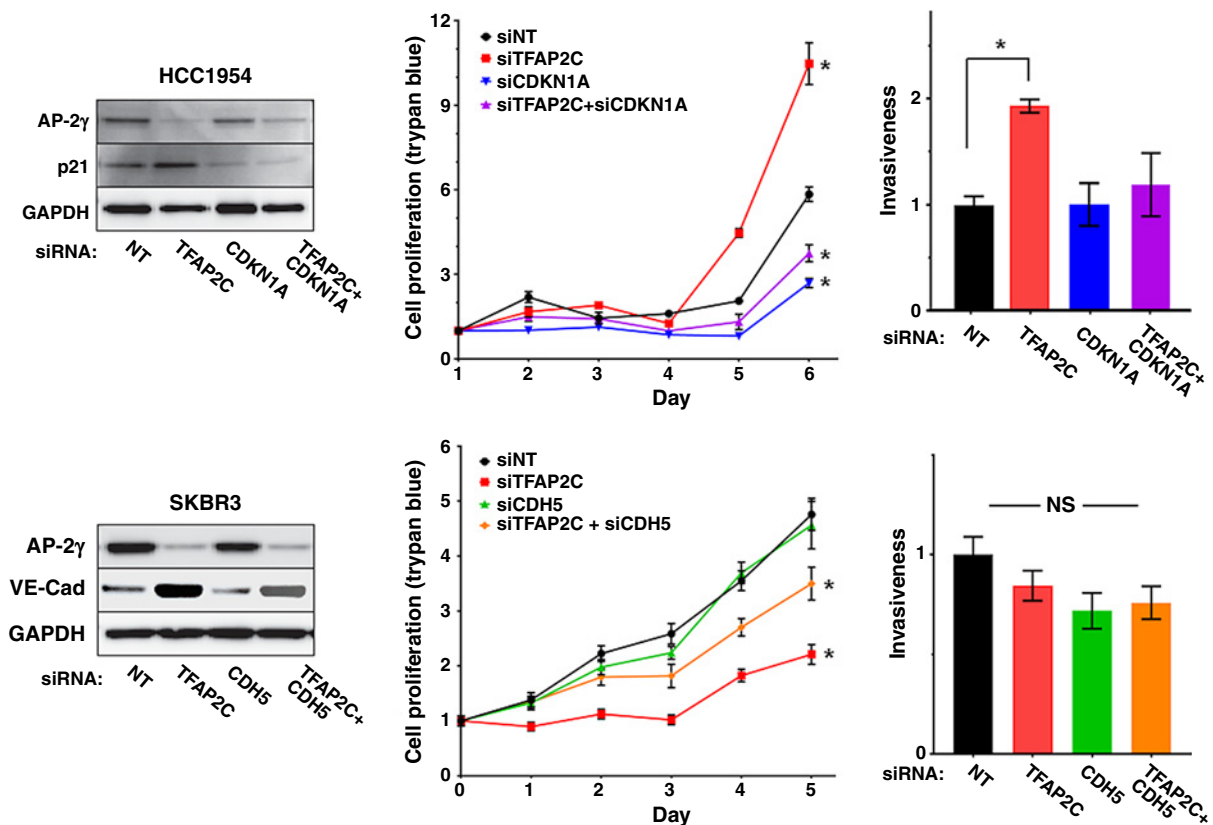
Wu et al.

**Figure 3.**

Summary of RNA-seq data with knockdown of *TFAP2C*. Significant changes in gene expression were first compared in HCC1954 with siRNA or shRNA-stable knockdown. The 152 genes with significant and consistent changes were compared with knockdown of *TFAP2C* in SKBR3 cells with siRNA. Similarly, regulated genes (on left) and differentially regulated genes (on right) are summarized with intensity of color, indicating direction and magnitude of gene-expression changes.

**Figure 4.**

Expression of proteins of differentially regulated AP-2 $\gamma$ -responsive genes. **A**, Western blots for AP-2 $\gamma$ , VE-cadherin and p21 in HCC1954 and SKBR3 with knockdown of *TFAP2C* compared with NT. **B**, Western blots for protein expression in HCC1954 with stable knockdown comparing shRNA for NT versus *TFAP2C*. **C**, Select Western blots of additional AP-2 $\gamma$ -responsive genes in HCC1954. **D**, Immunofluorescence staining for p21 in HCC1954 and SKBR3 demonstrates cytoplasmic localization.

**Figure 5.**

Response of proliferation and invasiveness to *CDKN1A* and *CDH5*. HCC1954 cells (top) with knockdown of *TFAP2C*, *CDKN1A* or both; Western blots confirm knockdown of proteins (left); proliferation determined by counting viable cells (Trypan blue, middle); bar graph showing relative invasiveness in HCC1954 with knockdown of *TFAP2C* with or without knockdown of *CDKN1A* (right). Parallel experiments in SKBR3 cells (bottom) with knockdown of *TFAP2C*, *CDH5* or both; Western blots confirm knockdown (left); proliferation measured by viable cell counts (Trypan blue, middle); bar graph shows relative cell invasiveness (right). \*,  $P < 0.001$ .

### Mechanisms of gene regulation by TFAP2C

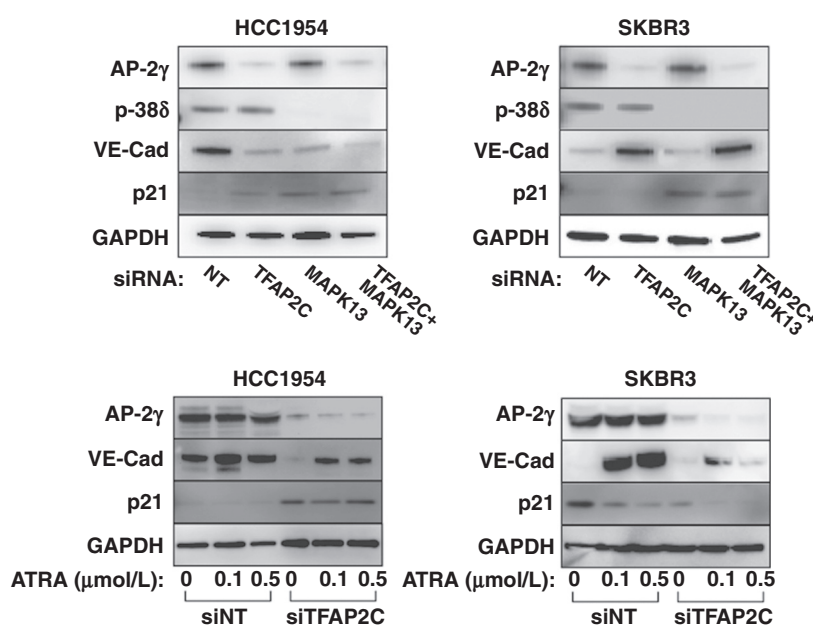
Because AP-2 $\gamma$  is a transcription factor, many of the changes in gene expression identified are thought to occur through altered transcription of AP-2 $\gamma$  target genes. The findings, however, may be due to genes that are both primary gene targets and secondary gene targets regulated through intermediary factor(s). ChIP-seq was performed in SKBR3 and HCC1954 to define potential differences in AP-2 $\gamma$  genomic occupancy. Most of the similarly regulated genes have patterns of occupancy that indicate primary targeting by AP-2 $\gamma$  in both SKBR3 and HCC1954. For example, the regulatory regions for *S100A7*, *CCL2*, *KRT15*, and *GDF15* demonstrate comparable patterns of AP-2 $\gamma$  occupancy (Supplementary Fig. S2). In evaluating the 68 differentially expressed genes, 31 (46%) had differential patterns of occupancy that could explain differences in regulation by *TFAP2C* knockdown. Examples of genes with differential occupancy of AP-2 $\gamma$  include *E2F2*, *RTN4R*, *RASL11A*, and *UST* (Supplementary Fig. S3). These differences in patterns of occupancy could be due to variations in epigenetic chromatin structure at regulatory regions that block AP-2 $\gamma$  occupancy, as previously demonstrated for the *GPX1* gene (26). On the other hand, 37 (54%) of the differentially regulated genes had patterns of AP-2 $\gamma$  occupancy that were comparable. For example, the regulatory regions of *CDKN1A*, *CDH5*, *IGFBP5*, and *S100A9* all have

similar patterns of AP-2 $\gamma$  occupancy in HCC1954 and SKBR3 (Supplementary Fig. S4). Although there were examples of slight differences in the comparative peak height in certain cases, the differences in patterns of occupancy were unlikely to account for differences in expression. Hence, differences in occupancy alone would not explain differential response to *TFAP2C* knockdown. To determine additional regulatory nodes that may be involved in the transcriptional pathways differentially regulated by AP-2 $\gamma$  in HER2<sup>+</sup> cell lines, the differentially regulated AP-2 $\gamma$  target genes were analyzed using the Ingenuity Pathway Analysis software (Supplementary Figs. S5 and S6). Two regulatory nodes were identified as potentially contributing to differential expression of the AP-2 $\gamma$  target genes: p38/MAPK and retinoic acid (Supplementary Figs. S5A and S6).

### Regulation by p38 $\delta$ /MAPK13

p38/MAPKs are a group of MAPKs that regulate responses to inflammation, oxidative stress, and several oncogenic properties involving tumor progression, including angiogenesis, invasion, and metastasis. The p38/MAPK family is composed of four isoforms encoded by separate genes: *p38 $\alpha$ /MAPK14*, *p38 $\beta$ /MAPK11*, *p38 $\gamma$ /MAPK12*, and *p38 $\delta$ /MAPK13* (27). To determine which isoform may be involved in differential response to AP-2 $\gamma$ , the expressions of

Wu et al.

**Figure 6.**

Expression of VE-cadherin and p21 in response to MAPK13 and ATRA. Western blots for AP-2γ, p38δ, VE-cadherin, p21 and GAPDH in HCC1954 and SKBR3 cells with knockdown of *TFAP2C* with or without co-knockdown of *MAPK13* (top). Western blots showing changes of expression of AP-2γ, VE-cadherin, p21, and GAPDH in HCC1954 and SKBR3 with knockdown using NT versus *TFAP2C* siRNA with increasing concentration of ATRA at 0, 0.1, and 0.5 μmol/L (bottom).

all four isoforms were examined in HCC1954 and SKBR3 with knockdown of *TFAP2C* (Supplementary Fig. S5B). Interestingly, the expression of *MAPK13* increased in HCC1954 and decreased in SKBR3 with *TFAP2C* knockdown, whereas, the other p38/MAPKs demonstrated no significant change (Supplementary Fig. S5B).

In HCC1954 knockdown of *MAPK13* repressed expression of VE-cadherin and increased that of p21, and these effects were comparable with the effects of *TFAP2C* knockdown (Fig. 6). These data suggest that effects on *CDH5* and *CDKN1A* expression with *TFAP2C* knockdown may be mediated through repression of *MAPK13* in HCC1954 cells. Conversely, knockdown of *MAPK13* in SKBR3 cells failed to demonstrate any effect on VE-cadherin expression; similar to effects in HCC1954, knockdown of *MAPK13* induced p21 expression in SKBR3, but this effect was opposite to knockdown of *TFAP2C* (Fig. 6). Overall, the data support the conclusion that in HCC1954, p38δ represents a regulatory node that contributes to the regulation of *CDH5* and *CDKN1A* with knockdown of *TFAP2C*. However, in SKBR3, knockdown of *MAPK13* does not reproduce the effect of *TFAP2C* knockdown, indicating that either p38/MAPK13 is not involved or p38δ activity is upregulated by knockdown of *TFAP2C*. In either case, activity of p38δ appears to be a candidate regulatory node contributing to the differential expression of *CDH5* and *CDKN1A* in HER2<sup>+</sup> cell lines.

#### Regulation by retinoic acid/ATRA

To examine the potential role of retinoic acid signaling, the effect of ATRA was examined in the HER2<sup>+</sup> cell lines with and without knockdown of *TFAP2C* (Fig. 6). In SKBR3, ATRA induced VE-cadherin levels by 35-fold and repressed p21 expression, responses that were similar to the effects of *TFAP2C* knockdown, which significantly blunted the response to ATRA treatment. In HCC1954 ATRA had insignificant effects on VE-cadherin and p21 expression, although with *TFAP2C* knockdown, there was a modest induction of VE-cadherin from the lower baseline expression. Therefore, SKBR3 cells were more responsive to ATRA with significant changes in the expression of both VE-cadherin and p21 that mirrored the effects of *TFAP2C* knockdown. Retinoic acid response in HCC1954 was negligible in the presence of *TFAP2C* expression. The findings suggest that

p38δ is an important regulatory node for the AP-2γ pathway in HCC1954 cells and that retinoic acid is a more important regulatory node in SKBR3 cells. Differences in the involvement of these two regulatory nodes may account for differential effects of *TFAP2C* knockdown.

#### Use of the gene signature to predict outcome in HER2 breast cancer

The set of genes differentially expressed with knockdown of *TFAP2C* comparing HCC1954 and SKBR3 are implicated in the growth and invasiveness of HER2<sup>+</sup> breast cancer. The clinical importance of the gene signature based on the differentially expressed genes was analyzed by examining an association between the expression of the gene set and outcome in patients with breast cancer. Regression analysis was used to establish a correlation between expression of the differentially regulated genes and outcome using datasets with gene expression data linked to clinical outcome. The Yau and colleagues (19) dataset had data for 69 patients with HER2<sup>+</sup> breast cancer with distant metastasis-free survival (DMFS) that included expression data for 41 of the 68 genes in our gene signature. Using regression analysis, there were 10 genes that demonstrated HRs with statistical significance (Supplementary Fig. S7), with 7 genes associated with a low HR (*ACSL1*, *CDH5*, *DCBLD2*, *FOXD1*, *KCNK5*, *MGP*, *RHEB*) and three genes associated with a high HR (*CDC42EP1*, *HOXB9*, *STEAP4*). A model was developed to create a recurrence score (RS) using the expression of all 41 genes with high or low RS based on values above or below the median (Supplementary Data; Supplementary Table S1). There was a striking difference in DMFS comparing high versus low RS in ER<sup>-</sup>/HER2<sup>+</sup> tumors (Fig. 7). When the model was applied to other tumor subtypes, patients with ER<sup>+</sup>/HER2<sup>+</sup> tumors also demonstrated a significant predictive capacity for high versus low RS. However, when applied to HER2<sup>-</sup> tumor subtypes, the model failed to demonstrate significant differences for high versus low RS (Fig. 7). Although the regression model was developed on the basis of the expression of the gene set, the expression of individual genes (e.g., *CDH5* and *STEAP4*) was examined on the basis of relative gene expression level above (high) or below (low) the median. As

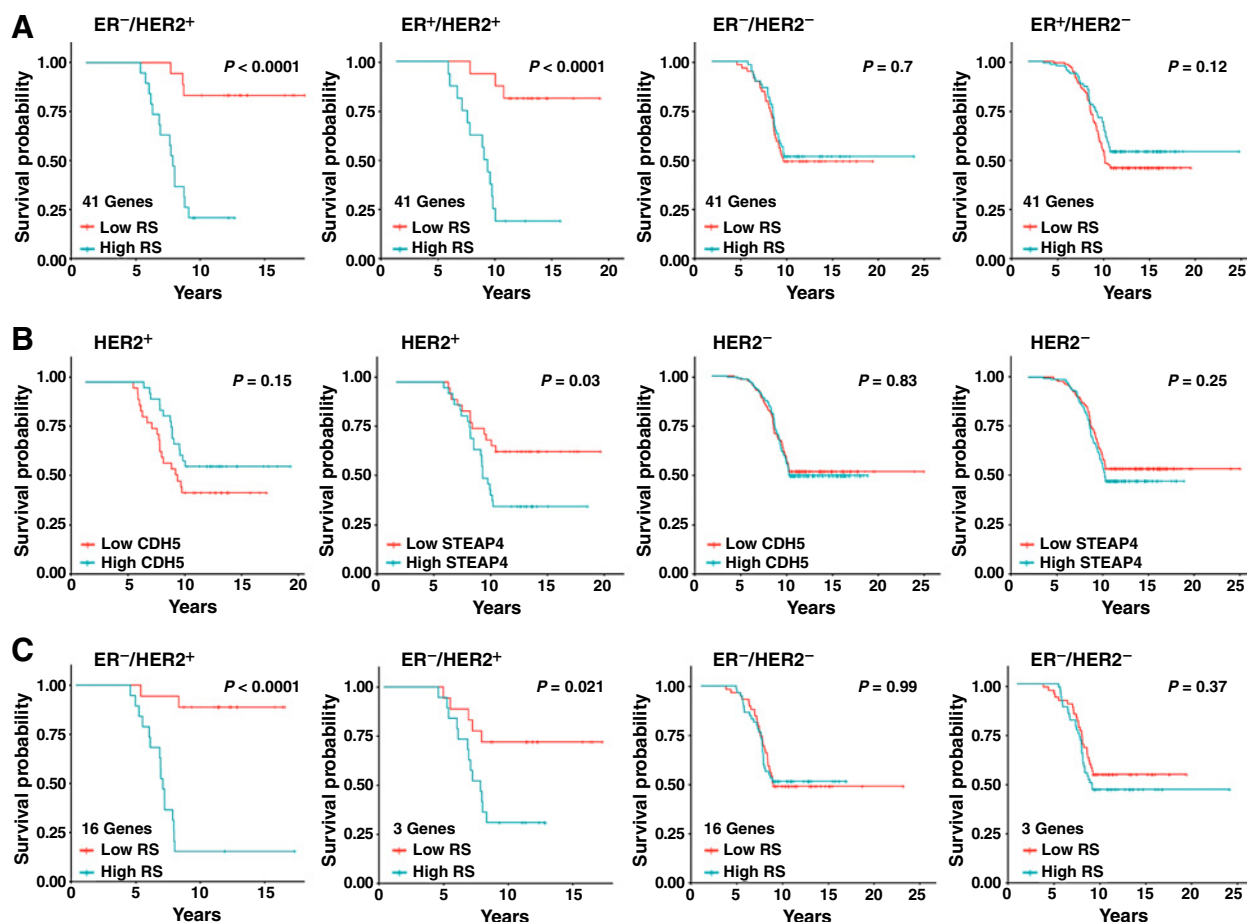


**Figure 7.**

Kaplan-Meier Plots for DMFS based on recurrence score model. **A**, Using the model with the 41-gene panel, Kaplan-Meier plots for DMFS for patients with each tumor subtypes as shown. For ER<sup>-</sup>/HER2<sup>+</sup>  $n = 37$ , ER<sup>+</sup>/HER2<sup>+</sup>  $n = 32$ , ER<sup>-</sup>/HER2<sup>-</sup>  $n = 119$ , ER<sup>+</sup>/HER2<sup>-</sup>  $n = 266$ . **B**, Examples of Kaplan-Meier plots for DMFS for individual genes, *CDH5* and *STEAP4*, for HER2<sup>+</sup> and HER2<sup>-</sup> tumors (with any ER status). **C**, Kaplan-Meier plots for DMFS using the model with 16-gene and 3-gene panels for ER<sup>-</sup>/HER2<sup>+</sup> and ER<sup>-</sup>/HER2<sup>-</sup> patients, as indicated.

predicted by the model, high *CDH5* expression was associated with better outcome, whereas, high *STEAP4* expression was associated with worse DMFS in patients with HER2<sup>+</sup> tumors (Fig. 7). On the other hand, no differences in DMFS were found in patients with HER2<sup>-</sup> tumors (Fig. 7).

In an attempt to further reduce the number of genes in the regression model, AP-2 $\gamma$  target genes were identified in a third HER2<sup>+</sup> breast cancer line, HCC1569. As described above, siRNA was used to knockdown *TFAP2C* expression compared with NT siRNA and RNA-seq analysis was used to identify significant changes in gene expression. Genes with significant changes in expression with *TFAP2C* knockdown in HCC1569 were compared with the 68 differentially expressed *TFAP2C* target genes; 32 of the 68 AP-2 $\gamma$  target genes were found to be significantly altered in HCC1569. Of these 32 genes, 16 genes were contained within the 41 genes available in the Yau and colleagues (19) dataset. A regression model was built based on these 16 AP-2 $\gamma$  target genes (Supplementary Data; Supplementary Table S2). The RS based on the 16-gene model was highly predictive of DMFS in ER<sup>-</sup>/HER2<sup>+</sup> patients (Fig. 7, bottom row); however, there was no difference in DMFS in ER<sup>-</sup>/HER2<sup>-</sup> patients. Regression analysis indicated that three genes (*ICK*, *KCNQ1*, and *STEAP4*) in the 16-gene panel were

independently significant (Supplementary Table S2). A model built using these three genes was also highly predictive of DMFS in ER<sup>-</sup>/HER2<sup>+</sup> patients but not in ER<sup>-</sup>/HER2<sup>-</sup> patients. These findings provide additional evidence that the AP-2 $\gamma$  target genes identified in the HER2<sup>+</sup> breast cancer model as likely involved in growth and invasion are predictive of outcome in patients with HER2<sup>+</sup> breast cancer.

## Discussion

Several previous studies of breast cancer have developed gene signatures that are predictive of outcome and in some cases can predict response to chemotherapy (22, 28). In addition, molecular profiling has been able to select patients that are less likely to benefit from adjuvant chemotherapy, thus avoiding unnecessary treatment (28, 29). Many of the gene signature models developed have been focused on ER $\alpha$ -positive breast cancer. In some cases, gene signature models that perform well in ER $\alpha$ <sup>+</sup>/HER2<sup>+</sup> patients do not have predictive capacity in the ER $\alpha$ <sup>-</sup>/HER2<sup>+</sup> breast cancer subtype (30). The HER2<sup>+</sup> breast cancer subtype has a poor prognosis relative to other intrinsic breast cancer subtypes (31). Hence, development of molecular profiles for the

Wu et al.

HER2<sup>+</sup> breast cancer subtype will help to stratify patients more likely to benefit from additional therapy and will further define pathways that can be targeted by directed therapy. This study is unique from several perspectives. Previous gene expression signatures were developed by using unsupervised hierarchical clustering algorithms to define similarities in patterns of expression to create associations with clinical phenotypes. This model was developed by defining a gene signature based on a set of genes likely to be associated with growth and invasion in HER2<sup>+</sup> breast cancer cell lines. Furthermore, other models in common use are more appropriate for ER $\alpha$ <sup>+</sup> tumors, whereas, the current model was developed specifically for application to the HER2<sup>+</sup> breast cancer subtype. The associations between outcome in patients with the HER2<sup>+</sup> breast cancer subtype and the gene expression signature described herein support the clinical relevance of the gene signature and the likelihood that the identified genes drive cancer cell growth and invasiveness.

Studies examining cell growth and invasiveness indicate that VE-cadherin/*CDH5* and p21/*CDKN1A* influence the growth and progression of HER2<sup>+</sup> breast cancer. Within the normal mammary gland, *CDH5* is expressed in the basal cell lineage within the quiescent mammary stem cell population that demonstrate multipotency and the capacity to develop mammary ducts (32). Studies of the role of VE-cadherin in cancer have resulted in conflicting findings, suggesting that VE-cadherin may have opposing effects depending upon the cancer type. In melanoma, VE-cadherin is overexpressed in aggressive subtypes and is involved in angiogenesis and formation of vascular-like networks mimicking embryonic vascular networks (33, 34). EMT is associated with “cadherin switching” characterized by downregulation of E-cadherin/*CDH1* and upregulation of both N-cadherin/*CDH2* and VE-cadherin/*CDH5* (33, 35). High expression of VE-cadherin/*CDH5* was reported to be associated with recurrence and the development of metastatic disease in breast cancer (36) and gastric cancer (37). However, knockdown of *CDH5* in MCF-7 luminal breast cancer cells increased cell invasiveness, suggesting that VE-cadherin suppresses metastatic potential (38). Our data support the finding that VE-cadherin/*CDH5* reduces cell growth and invasiveness in the HER2<sup>+</sup> breast cancer subtype.

P21 is a cyclin-dependent kinase inhibitor and induction of p21 normally leads to cell-cycle arrest and inhibition of proliferation (39). However, p21 can also inhibit apoptosis and, within certain contexts, p21 can paradoxically promote cell proliferation and tumor growth (40, 41). The paradoxical effects of p21 promoting cell proliferation, tumorigenicity, and invasiveness have been attributed to either its subcellular localization or deficiency of p53 (42, 43). Our findings that knockdown of *CDKN1A* repressed cell growth in certain HER2<sup>+</sup> breast cancer cells were corroborated by published experiments in AU565 cells (44). The potential role of p21 inducing cell proliferation and invasiveness in breast cancer is further supported by clinical studies showing that high p21 expression is associated with high tumor grade and advanced stage in patients with breast cancer (45). Also consistent with our findings, the worst 5-year survival rate was associated with high HER2 expression and cytoplasmic p21 localization (46).

The differential effects of AP-2 $\gamma$  in HCC1954 and SKBR3 were mirrored by a divergence in response to key regulatory pathways. In HCC1954 cells, knockdown of *TFAP2C* and *MAPK13* induced identical changes in the expression of *CDH5* and *CDKN1A*. Emerging data indicate an important role for *MAPK13*/p38 $\delta$  in several physiologic processes and oncogenesis. Studies in different cancer models have uncovered both oncogenic and tumor-suppressor functions of p38 $\delta$  dependent on the cell type. In breast cancer, overexpression of p38 $\delta$  is

associated with a worse prognosis, and knockdown of *MAPK13* in MCF-7 and MDA-MB-231 breast cancer cells reduced proliferation and decreased cell detachment (47). High expression of *MAPK13*/p38 $\delta$  was identified in a variety of cancer cell types, including gynecologic cancers where expression of p38 $\delta$  was required to maintain the cancer stem cell (CSC)/tumor-initiating cell (TIC) population (48). In contrast, the opposite findings were described in non-small cell lung cancer where p38 $\delta$  repressed cancer stem cell markers and inhibited the tumor cell-initiating ability (49). In this study, knockdown of *MAPK13* in HCC1954 cells induced alterations in *CDH5* and *CDKN1A* expression that mirrored changes with knockdown of *TFAP2C*, supporting a tumor inhibitory role in this cell line.

The retinoic acid pathway was identified as an important regulatory node that demonstrated differential activation in HER2<sup>+</sup> breast cancer cell lines. In SKBR-3 cells, ATRA induced *CDH5* and repressed *CDKN1A*, which mirrored effects of *TFAP2C* knockdown. Furthermore, the effects of ATRA were significantly dependent upon AP-2 $\gamma$ , because knockdown of *TFAP2C* blunted the effects of ATRA. These findings are in agreement with previous studies reporting that ATRA reduced proliferation and invasiveness of SKBR3 and MCF-7 cells (50, 51). In SKBR3 cells, ATRA activates a mammary epithelial differentiation program that decreased migration of cells with increased formation of adherens junctions involving upregulation of *CDH5*, whereas HCC1954 cells are relatively resistant to the action of ATRA (52). The current findings demonstrate that response to ATRA in SKBR3 cells is dependent upon AP-2 $\gamma$ , consistent with earlier findings that AP-2 $\gamma$  regulates genes in the retinoic acid response pathway in MCF-7 cells (7).

In conclusion, *TFAP2C* knockdown in the HER2<sup>+</sup> breast cancer subtype demonstrated cell-specific differences that were characterized by a set of differentially regulated AP-2 $\gamma$  target genes, which are involved in cell proliferation and invasion. Retinoic acid and *MAPK13*/p38 $\delta$  represent two regulatory nodes that demonstrated differential responses that mirror knockdown of *TFAP2C*. These findings suggest that HER2<sup>+</sup> breast cancers may be characterized by their sensitivity to retinoic acid and MAPK inhibitors, which may offer new therapeutic options for different subsets of patients with HER2<sup>+</sup> breast cancer. Further work will be needed to define patterns of expression that might predict response to either retinoic acid or MAPK inhibitor.

### Disclosure of Potential Conflicts of Interest

T.A. Braun is a consultant and director of Bioinformatics at Immortagene and scientific advisor Bio:Neos. No potential conflicts of interest were disclosed by the other authors.

### Authors' Contributions

**Conception and design:** V.T. Wu, B. Kiriazov, V.W. Gu, V. Band, H. Band, R.J. Weigel

**Development of methodology:** V.T. Wu, B. Kiriazov, V.W. Gu, W. Zhang, M.V. Kulak, R.J. Weigel

**Acquisition of data (provided animals, acquired and managed patients, provided facilities, etc.):** B. Kiriazov, K.E. Koch, A.C. Beck, P. Addo, Z.J. Wehrspan, T.A. Braun, M.V. Kulak, R.J. Weigel

**Analysis and interpretation of data (e.g., statistical analysis, biostatistics, computational analysis):** V.T. Wu, B. Kiriazov, K.E. Koch, V.W. Gu, A.C. Beck, N. Borcherding, T. Li, W. Zhang, T.A. Braun, B.J. Brown, M.V. Kulak, R.J. Weigel

**Writing, review, and/or revision of the manuscript:** V.T. Wu, B. Kiriazov, K.E. Koch, V.W. Gu, A.C. Beck, T. Li, Z.J. Wehrspan, W. Zhang, T.A. Braun, V. Band, H. Band, M.V. Kulak, R.J. Weigel

**Administrative, technical, or material support (i.e., reporting or organizing data, constructing databases):** B. Kiriazov, K.E. Koch, V.W. Gu, T.A. Braun, M.V. Kulak, R.J. Weigel

**Study supervision:** B. Kiriazov, R.J. Weigel

## Acknowledgments

This work was supported by the NIH grants R01CA183702 and T32CA148062 (PI: R.J. Weigel), P30CA0868218S6 (principal investigator: G.J.W.) and by a generous gift from the Kristen Olewine Milke Breast Cancer Research Fund. V.T. Wu, B. Kiriazov, K.E. Koch, and A.C. Beck were supported by the NIH grant T32CA148062.

## References

- Weigel RJ, deConinck EC. Transcriptional control of estrogen receptor in estrogen receptor-negative breast carcinoma. *Cancer Res* 1993;53:3472–4.
- deConinck EC, McPherson LA, Weigel RJ. Transcriptional regulation of estrogen receptor in breast carcinomas. *Mol Cell Biol* 1995;15:2191–6.
- McPherson LA, Baichwal VR, Weigel RJ. Identification of ERF-1 as a member of the AP2 transcription factor family. *Proc Natl Acad Sci U S A* 1997;94:4342–7.
- Woodfield GW, Horan AD, Chen Y, Weigel RJ. TFAP2C controls hormone response in breast cancer cells through multiple pathways of estrogen signaling. *Cancer Res* 2007;67:8439–43.
- Kang HJ, Lee MH, Kang HL, Kim SH, Ahn JR, Na H, et al. Differential regulation of estrogen receptor alpha expression in breast cancer cells by metastasis-associated protein 1. *Cancer Res* 2014;74:1484–94.
- Bogachek MV, Chen Y, Kulak MV, Woodfield GW, Cyr AR, Park JM, et al. Sumoylation pathway is required to maintain the Basal breast cancer subtype. *Cancer Cell* 2014;25:748–61.
- Woodfield GW, Chen Y, Bair TB, Domann FE, Weigel RJ. Identification of primary gene targets of TFAP2C in hormone responsive breast carcinoma cells. *Genes Chromosomes Cancer* 2010;49:948–62.
- Tan SK, Lin ZH, Chang CW, Varang V, Chng KR, Pan YF, et al. AP-2gamma regulates estrogen receptor-mediated long-range chromatin interaction and gene transcription. *EMBO J* 2011;30:2569–81.
- Gee JM, Eloranta JJ, Ibbitt JC, Robertson JF, Ellis IO, Williams T, et al. Overexpression of TFAP2C in invasive breast cancer correlates with a poorer response to anti-hormone therapy and reduced patient survival. *J Pathol* 2009;217:32–41.
- Perkins SM, Bales C, Vladislav T, Althouse S, Miller KD, Sandusky G, et al. TFAP2C expression in breast cancer: correlation with overall survival beyond 10 years of initial diagnosis. *Breast Cancer Res Treat* 2015;152:519–31.
- Cyr AR, Kulak MV, Park JM, Bogachek MV, Spanheimer PM, Woodfield GW, et al. TFAP2C governs the luminal epithelial phenotype in mammary development and carcinogenesis. *Oncogene* 2015;34:436–44.
- Bosher JM, Williams T, Hurst HC. The developmentally regulated transcription factor AP-2 is involved in c-erbB-2 overexpression in human mammary carcinoma. *Proc Natl Acad Sci U S A* 1995;92:744–7.
- Delacroix L, Begon D, Chatel G, Jackers P, Winkler R. Distal ERBB2 promoter fragment displays specific transcriptional and nuclear binding activities in ERBB2 overexpressing breast cancer cells. *DNA Cell Biol* 2005;24:582–94.
- Ailan H, Xiangwen X, Daolong R, Lu G, Xiaofeng D, Xi Q, et al. Identification of target genes of transcription factor activator protein 2 gamma in breast cancer cells. *BMC Cancer* 2009;9:279.
- Nolens G, Pignon JC, Koopmansch B, Elmoualij B, Zorzi W, De Pauw E, et al. Ku proteins interact with activator protein-2 transcription factors and contribute to ERBB2 overexpression in breast cancer cell lines. *Breast Cancer Res* 2009;11:R83.
- Liu Q, Kulak MV, Borcharding N, Maina PK, Zhang W, Weigel RJ, et al. A novel HER2 gene body enhancer contributes to HER2 expression. *Oncogene* 2018;37:687–94.
- Prat A, Perou CM. Deconstructing the molecular portraits of breast cancer. *Mol Oncol* 2011;5:5–23.
- Shiu KK, Wetterskog D, Mackay A, Natrajan R, Lambros M, Sims D, et al. Integrative molecular and functional profiling of ERBB2-amplified breast cancers identifies new genetic dependencies. *Oncogene* 2014;33:619–31.
- Yau C, Esserman L, Moore DH, Waldman F, Sninsky J, Benz CC. A multigene predictor of metastatic outcome in early stage hormone receptor-negative and triple-negative breast cancer. *Breast Cancer Res* 2010;12:R85.
- Klonowska K, Czubak K, Wojciechowska M, Handschuh L, Zmienko A, Figlerowicz M, et al. Oncogenomic portals for the visualization and analysis of genome-wide cancer data. *Oncotarget* 2016;7:176–92.
- Therneau TM. A package for survival analysis in S. version 2.38; 2015. Available from: <https://CRAN.R-project.org/package=survival>.
- Paik S, Shak S, Tang G, Kim C, Baker J, Cronin M, et al. A multigene assay to predict recurrence of tamoxifen-treated, node-negative breast cancer. *N Engl J Med* 2004;351:2817–26.
- Kassambara A, Kosinski M. Survminer: drawing survival curves using ggplot2. 2018. Available from: <http://www.sthda.com/english/rpkgs/survminer/>.
- Chang TH, Tsai MF, Gow CH, Wu SG, Liu YN, Chang YL, et al. Upregulation of microRNA-137 expression by Slug promotes tumor invasion and metastasis of non-small cell lung cancer cells through suppression of TFAP2C. *Cancer Lett* 2017;402:190–202.
- Zhou BP, Liao Y, Xia W, Spohn B, Lee MH, Hung MC. Cytoplasmic localization of p21Cip1/WAF1 by Akt-induced phosphorylation in HER-2/neu-overexpressing cells. *Nat Cell Biol* 2001;3:245–52.
- Kulak MV, Cyr AR, Woodfield GW, Bogachek M, Spanheimer PM, Li T, et al. Transcriptional regulation of the GPX1 gene by TFAP2C and aberrant CpG methylation in human breast cancer. *Oncogene* 2013;32:4043–51.
- Cuenda A, Sanz-Ezquerro JJ. p38gamma and p38delta: from spectators to key physiological players. *Trends Biochem Sci* 2017;42:431–42.
- Cardoso F, van't Veer LJ, Bogaerts J, Slaets L, Viale G, Delaloge S, et al. 70-gene signature as an aid to treatment decisions in early-stage breast cancer. *N Engl J Med* 2016;375:717–29.
- Sparano JA, Gray RJ, Makower DF, Pritchard KI, Albain KS, Hayes DF, et al. Prospective validation of a 21-gene expression assay in breast cancer. *N Engl J Med* 2015;373:2005–14.
- Risi E, Grilli A, Migliaccio I, Biagioni C, McCartney A, Guarducci C, et al. A gene expression signature of Retinoblastoma loss-of-function predicts resistance to neoadjuvant chemotherapy in ER-positive/HER2-positive breast cancer patients. *Breast Cancer Res Treat* 2018;170:329–41.
- Sorlie T, Perou CM, Tibshirani R, Aas T, Geisler S, Johnsen H, et al. Gene expression patterns of breast carcinomas distinguish tumor subclasses with clinical implications. *Proc Natl Acad Sci U S A* 2001;98:10869–74.
- Sun H, Miao Z, Zhang X, Chan UI, Su SM, Guo S, et al. Single-cell RNA-Seq reveals cell heterogeneity and hierarchy within mouse mammary epithelia. *J Biol Chem* 2018;293:8315–29.
- Berx G, van Roy F. Involvement of members of the cadherin superfamily in cancer. *Cold Spring Harb Perspect Biol* 2009;1:a003129.
- Hendrix MJ, Seftor EA, Meltzer PS, Gardner LM, Hess AR, Kirschmann DA, et al. Expression and functional significance of VE-cadherin in aggressive human melanoma cells: role in vasculogenic mimicry. *Proc Natl Acad Sci U S A* 2001;98:8018–23.
- Labelle M, Schnittler HJ, Aust DE, Friedrich K, Baretton G, Vestweber D, et al. Vascular endothelial cadherin promotes breast cancer progression via transforming growth factor beta signaling. *Cancer Res* 2008;68:1388–97.
- Fry SA, Robertson CE, Swann R, Dwek MV. Cadherin-5: a biomarker for metastatic breast cancer with optimum efficacy in estrogen receptor-positive breast cancers with vascular invasion. *Br J Cancer* 2016;114:1019–26.
- Inokuchi M, Higuchi K, Takagi Y, Tanioka T, Nakagawa M, Gokita K, et al. Cadherin 5 is a significant risk factor for hematogenous recurrence and a prognostic factor in locally advanced gastric cancer. *Anticancer Res* 2017;37:6807–13.
- Zheng L, Zhang Z, Zhang S, Guo Q, Zhang F, Gao L, et al. RNA binding protein RNPC1 inhibits breast cancer cell metastasis via activating STARD13-Related ceRNA network. *Mol Pharm* 2018;15:2123–32.
- Xiong Y, Hannon GJ, Zhang H, Casso D, Kobayashi R, Beach D. p21 is a universal inhibitor of cyclin kinases. *Nature* 1993;366:701–4.
- Abbas T, Dutta A. p21 in cancer: intricate networks and multiple activities. *Nat Rev Cancer* 2009;9:400–14.
- Gartel AL, Radhakrishnan SK. Lost in transcription: p21 repression, mechanisms, and consequences. *Cancer Res* 2005;65:3980–5.
- Zohny SF, Al-Malki AL, Zamzami MA, Choudhry H. p21(Waf1/Cip1): its paradoxical effect in the regulation of breast cancer. *Breast Cancer* 2018;26:131–7.
- Georgakilas AG, Martin OA, Bonner WM. p21: a two-faced genome guardian. *Trends Mol Med* 2017;23:310–9.

## Wu et al.

44. Chiang CT, Way TD, Lin JK. Sensitizing HER2-overexpressing cancer cells to luteolin-induced apoptosis through suppressing p21(WAF1/CIP1) expression with rapamycin. *Mol Cancer Ther* 2007;6:2127–38.
45. Zohny SF, Baothman OA, El-Shinawi M, Al-Malki AL, Zamzami MA, Choudhry H. The KIP/CIP family members p21<sup>Waf1/Cip1</sup> and p57<sup>Kip2</sup> as diagnostic markers for breast cancer. *Cancer Biomark* 2017;18:413–23.
46. Xia W, Chen JS, Zhou X, Sun PR, Lee DF, Liao Y, et al. Phosphorylation/cytoplasmic localization of p21Cip1/WAF1 is associated with HER2/neu over-expression and provides a novel combination predictor for poor prognosis in breast cancer patients. *Clin Cancer Res* 2004;10:3815–24.
47. Wada M, Canals D, Adada M, Coant N, Salama MF, Helke KL, et al. P38 delta MAPK promotes breast cancer progression and lung metastasis by enhancing cell proliferation and cell detachment. *Oncogene* 2017;36:6649–57.
48. Yasuda K, Hirohashi Y, Kuroda T, Takaya A, Kubo T, Kanaseki T, et al. MAPK13 is preferentially expressed in gynecological cancer stem cells and has a role in the tumor-initiation. *Biochem Biophys Res Commun* 2016;472:643–7.
49. Fang Y, Wang J, Wang G, Zhou C, Wang P, Zhao S, et al. Inactivation of p38 MAPK contributes to stem cell-like properties of non-small cell lung cancer. *Oncotarget* 2017;8:26702–17.
50. Vanderhoeven F, Redondo AL, Martinez AL, Vargas-Roig LM, Sanchez AM, Flamini MI. Synergistic antitumor activity by combining trastuzumab with retinoic acid in HER2 positive human breast cancer cells. *Oncotarget* 2018;9:26527–42.
51. Lin G, Zhu S, Wu Y, Song C, Wang W, Zhang Y, et al. Omega-3 free fatty acids and all-trans retinoic acid synergistically induce growth inhibition of three subtypes of breast cancer cell lines. *Sci Rep* 2017;7:2929.
52. Zanetti A, Affatato R, Centritto F, Fratelli M, Kurosaki M, Barzago MM, et al. All-trans-retinoic acid modulates the plasticity and inhibits the motility of breast cancer cells: role of NOTCH1 and transforming growth factor (TGFbeta). *J Biol Chem* 2015;290:17690–709.

# Molecular Cancer Research

## A *TFAP2C* Gene Signature Is Predictive of Outcome in HER2-Positive Breast Cancer

Vincent T. Wu, Boris Kiriazov, Kelsey E. Koch, et al.

*Mol Cancer Res* 2020;18:46-56. Published OnlineFirst October 16, 2019.

**Updated version** Access the most recent version of this article at:  
doi:[10.1158/1541-7786.MCR-19-0359](https://doi.org/10.1158/1541-7786.MCR-19-0359)

**Supplementary Material** Access the most recent supplemental material at:  
<http://mcr.aacrjournals.org/content/suppl/2019/10/16/1541-7786.MCR-19-0359.DC1>

**Cited articles** This article cites 50 articles, 17 of which you can access for free at:  
<http://mcr.aacrjournals.org/content/18/1/46.full#ref-list-1>

**E-mail alerts** [Sign up to receive free email-alerts](#) related to this article or journal.

**Reprints and Subscriptions** To order reprints of this article or to subscribe to the journal, contact the AACR Publications Department at [pubs@aacr.org](mailto:pubs@aacr.org).

**Permissions** To request permission to re-use all or part of this article, use this link  
<http://mcr.aacrjournals.org/content/18/1/46>.  
Click on "Request Permissions" which will take you to the Copyright Clearance Center's (CCC) Rightslink site.